

Raman spectra of lignin model compounds

UMESH P AGARWAL, RICHARD S REINER, ASHOK K PANDEY¹, SALLY A RALPH, KOLBY C HIRTH, AND RAJAI H ATALLA

USDAFS-Forest Products Laboratory, Madison WI 53726 USA

¹Tropical Forest Research Institute, P.O. RFRC, Mandla Road, Jabalpur 482 021 India

ABSTRACT

To fully exploit the value of Raman spectroscopy for analyzing lignins and lignin-containing materials, a detailed understanding of lignins' Raman spectra needs to be achieved. Although advances made thus far have led to significant growth in application of Raman techniques, further developments are needed to improve upon the existing knowledge. Considering that lignin's heterogeneous structure consists not only of inter-phenylpropane-unit linkages of carbon-to-carbon and carbon-to-oxygen, but also of side chains with various substituent and functional groups, a study of a large number of representative models is essential. In the present work, 40 lignin models were investigated in the neat state (near-IR FT-Raman and FT-IR), in solution (near-IR FT-Raman), and on cellulose (near-IR FT-Raman). These models represent a large number of substituent/functional groups and sub-structures in lignin - aliphatic and phenolic OH, C=O, CHO, COOH, CH₃, OCH₃, α,β C=C, furan, and interunit C-O-C and C-C linkages. Raman band positions associated with various groups were identified and Raman frequencies and intensities were compared between the models. For example, for the phenyl group, some of the noteworthy findings were as follows. The intensities of the 1600 (aromatic ring stretch) and 3070 (aromatic C-H stretch) cm⁻¹ bands varied significantly between the models. The position of the 1600 cm⁻¹-Raman-mode was found to be only minimally sensitive to substituents because in about 70 % of the models, including those containing more than 1 phenyl group, the vibrational frequency was confined between 1594 and 1603 cm⁻¹. Similar information was obtained on other functional groups as well. It is hoped that the findings from this study will greatly aid in developing a better understanding of the Raman spectra of lignins and lignocellulosic materials.

INTRODUCTION

Raman spectroscopy is increasingly used to analyze lignin containing materials [1-8]. Although significant progress has been made in interpreting the contribution of lignin to a spectrum [9], the need exists to further improve upon this understanding. This can be accomplished by carrying out a

systematic broad-based investigation of lignin models. Earlier work in this area focused on a few models that were deemed relevant to the study at hand. However, such investigations and resultant advances in understanding were not sufficient. Considering that lignin is a heterogeneous polymer that consists of many different types of inter-unit linkages, substituents, and side chains with various functional groups, a study incorporating a large number of representative models is essential. In the present work, using near-IR FT-Raman and FT-IR techniques, 40 lignin models (nearly half of them tri-substituted aromatics) were investigated in neat state. Additionally, near-IR FT-Raman was used to study these models in solution and on cellulose.

EXPERIMENTAL

Chemicals

A large number of lignin models (Fig. 1) were purchased from Aldrich, Eastman, Fluka, and Lancaster. Additionally, a significant number were synthesized by an FPL staff chemist (Larry Landucci). Model structures and their ID numbers are shown in Fig. 1

Raman- and IR- neat

Near-IR FT-Raman and FT-IR spectra of the pure models were obtained, respectively, using the RFS 100 (Bruker) and Galaxy-5000 (Mattson) instruments.

Raman- solution

Appropriate amounts of compounds were weighed in 1, 2 or 3 mL Class A volumetric flasks and dissolved in methanol, dioxane:water or dimethyl sulfoxide (DMSO) with most solutions near 0.5 M. For solution studies, most models were dissolved in methanol. For those few that were not soluble, dioxane:water or DMSO was used. The solvent background was subtracted from the raw data prior to determining peak positions and intensities. Peak intensity was calculated on a molar basis and for those models that contained more than one group per molecule the band intensity was adjusted by ratioing to the appropriate number of such groups.

Raman- cellulose

Solutions used above (with exceptions: 10, 16 and 19) were measured in a 1 mL GlenCo Precision Bore ampoule and luted with the appropriate solvent to make 0.5 mL of 0.1 M solutions. This was poured onto a 55 mm round Whatman #1 filter paper and allowed to evaporate for 2-5 days. The papers were folded into 16 layers and placed on the sampling bench in the instrument with a mirror behind them. Model peaks that occurred in essentially the same place as cellulose peaks were not included in the results because there would be significant uncertainty regarding the peak position and amplitude

	R ₁	R ₂	R ₃	R ₄
1	-COOH	-H	-OCH ₃	-H
2	-COOH	-OCH ₃	-OCH ₃	-H
3	-CH=CHCHO	-H	-OCH ₃	-H
4	-H	-OCH ₃	-OH	-OCH ₃
5	$\begin{matrix} \text{O} \\ \\ -\text{CCH}_3 \end{matrix}$	-OCH ₃	-OCH ₃	-H
6	$\begin{matrix} \text{O} \\ \\ -\text{CCH}_3 \end{matrix}$	-OCH ₃	-OH	-H
7	<i>figure</i>	-H	-H	-H
8	-CH=CHCOOH	-H	-OCH ₃	-H
9	-H	-OCH ₃	-OCH ₃	-H
10	$\begin{matrix} \text{O} \\ \\ -\text{CCH}_3 \end{matrix}$	-OCH ₃	$\begin{matrix} \text{O} \\ \\ -\text{OCCH}_3 \end{matrix}$	-H
11	$\begin{matrix} \text{O} \\ \\ -\text{CCH}_3 \end{matrix}$	-H	-H	-H
12	-CHO	-OCH ₃	-OCH ₃	-H
13	$\begin{matrix} \text{O} \\ \\ -\text{CCH}_3 \end{matrix}$	-H	-OH	-H
14	-CH=CHCOOH	-OCH ₃	-OH	-H
15	$\begin{matrix} \text{O} \\ \\ -\text{CCH}_3 \end{matrix}$	-OCH ₃	-OCH ₃	-OCH ₃
16	<i>figure</i>	-OCH ₃	-OH	-H
17	-CH=CHCOOH	-OCH ₃	-OH	-OCH ₃
18	-CH ₂ OH	-H	-OH	-H
19	<i>figure</i>	-H	<i>figure</i>	-H
20	$\begin{matrix} \text{O} \\ \\ -\text{CCH}_3 \end{matrix}$	-H	<i>figure</i>	-H

	R ₁	R ₂	R ₃	R ₄
21	$\begin{matrix} \text{O} \\ \\ -\text{CCH}_2\text{CH}_3 \end{matrix}$	-OCH ₃	-OH	-OCH ₃
22	<i>figure</i>	-OCH ₃	-OCH ₃	-H
23	<i>figure</i>	-OCH ₃	-OH	-H
24	<i>figure</i>	-OCH ₃	-OCH ₃	-H
25	$\begin{matrix} \text{OH} \\ \\ -\text{CHCH}_3 \end{matrix}$	-OCH ₃	-OCH ₃	-H
26	-CH ₃	-OCH ₃	-OH	-H
27	-CH ₂ OH	-OCH ₃	-OCH ₃	-H
28	-CH ₃	-OCH ₃	$\begin{matrix} \text{O} \\ \\ -\text{OCCH}_3 \end{matrix}$	-H
29	-CH ₂ OH	-H	-OCH ₃	-H
30	-CH ₂ CH ₂ CH ₃	-OCH ₃	-OH	-H
31	-CH=CHCH ₃	-OCH ₃	-OH	-H
32	-COOH	-OCH ₃	-OH	-H
33	-CHO	-OH	-OCH ₃	-H
34	-CHO	-OCH ₃	-OH	-H
35	-COOH	-OCH ₃	-OH	-OCH ₃
36	-CHO	-OCH ₃	-OH	-OCH ₃
37	-CH=CHCOOH	-H	-OH	-H
38	-COOH	-H	-OH	-H
39	-CHO	-OCH ₃	-OCH ₃	-OCH ₃
40	$\begin{matrix} \text{O} \\ \\ -\text{CCH}_3 \end{matrix}$	-OCH ₃	-OH	-OCH ₃

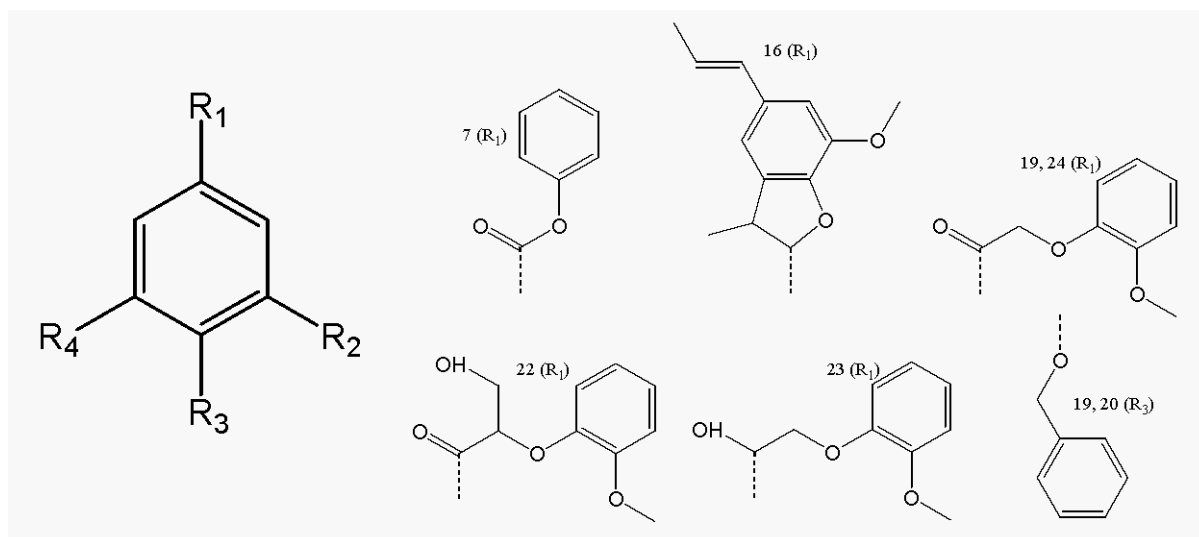


Fig. 1: Molecular structures of 40 lignin models used in the present study

Table 1: Raman band positions of lignin models in 3 environments - neat, in solution, and on cellulose

Sample	Most prominent bands																							
	824	1134	1180	1270	1291	1452	1581	1609	3029	3079	634	823	1181	1269	1290	1452	1580	1608	3029	3078				
1	Neat	WN*	824	1134	1180	1270	1291	1452	1581	1609	3029	3079	634	823	1181	1269	1290	1452	1580	1608	3029	3078		
		Cell	WN										634	819	1258									
		Soln	WN																					
2	Neat	WN	357	745	771	1268	1296	1352	1438	1454	1598	3088	353	628	744	770	1253	1354	1414	1599	3089			
		Cell	WN																					
		Soln	WN																					
3	Neat	WN	568	1131	1174	1250	1406	1570	1600	1621	1664	1675	568	639	767	1136	1176	1251	1571	1599	1623	1660		
		Cell	WN																					
		Soln	WN																					
4	Neat	WN	368	531	708	823	1084	1297	1460	1592	3075	3090	368	531	708	823	1084	1297	1460	1592	3075	3090		
		Cell	WN																					
		Soln	WN																					
5	Neat	WN	765	979	1082	1266	1347	1418	1446	1587	1671	3080	677	768	1271	1419	1452	1595	1667	3083				
		Cell	WN																					
		Soln	WN																					
6	Neat	WN	342	366	684	1079	1162	1188	1288	1577	1606	1659	342	366	684	1079	1162	1188	1288	1577	1606	1659		
		Cell	WN																					
		Soln	WN																					
7	Neat	WN	263	856	1003	1028	1170	1194	1264	1600	1727	3070	263	856	1003	1028	1170	1194	1264	1600	1727	3070		
		Cell	WN																					
		Soln	WN																					
8	Neat	WN	815	1178	1241	1273	1433	1464	1602	1629	3061	3079	775	861	1174	1194	1213	1265	1307	1422	1604	1638		
		Cell	WN																					
		Soln	WN																					
9	Neat	WN	380	581	753	1053	1163	1255	1332	1457	1594	3078	380	581	753	1053	1163	1255	1332	1457	1594	3078		
		Cell	WN																					
		Soln	WN																					
10	Neat	WN	314	355	667	747	804	1291	1328	1607	1625	3086	314	355	667	747	804	1291	1328	1607	1625	3086		
		Cell	WN																					
		Soln	WN																					
11	Neat	WN	288	722	1000	1029	1150	1279	1597	1650	3059	3068	288	722	1000	1029	1150	1279	1597	1650	3059	3068		
		Cell	WN																					
		Soln	WN																					
12	Neat	WN	377	643	734	773	1198	1278	1350	1445	1599	1672	3079	377	643	734	773	1198	1278	1350	1445	1599	1672	3079
		Cell	WN																					
		Soln	WN																					
13	Neat	WN	638	842	962	1077	1165	1219	1276	1575	1604	1660	638	842	962	1077	1165	1219	1276	1575	1604	1660		
		Cell	WN																					
		Soln	WN																					

Soln WN	638	823	842	962	1076	1171	1279	1584	1606	1663	3073
14 Neat WN	396	673	815	1178	1241	1273	1433	1464	1602	1629	
Cell WN		810	1188	1276	1430	1452	1600	1630	1679	3070	
Soln WN		812	1162	1191	1223	1274	1431	1455	1603	1633	1687
15 Neat WN	376	752	890	980	995	1035	1093	1216	1322	1452	1586
Cell WN		608	751	889	980	995		1216	1325	1451	1585
Soln WN		743				1098			1333		1585
16 Neat WN		790		913	1075		1274	1322	1338	1386	1455
Cell WN			811						1336		1450
Soln WN	756				1145	1191			1338	1379	1601
17 Neat WN		1160	1209	1271	1305	1336	1425	1459	1516	1595	1644
Cell WN	814							1514	1594	1632	1676
Soln WN		1161				1337			1595	1635	1688
18 Neat WN	406	644	827	853	995	1172	1211	1599	1613	3065	
Cell WN		642	828	849			1600	1614	3063		
Soln WN		642	824	849		1170	1209	1617	3063		
19 Neat WN	754	767	1007	1192	1248	1264	1346	1451	1596	1687	
Cell WN	753	771	1003					1594	1690	3066	
Soln WN	755	771	1002	1201		1267	1334	1594	1691	3062	
20 Neat WN		863		1005	1077	1173	1250		1303	1600	1672
Cell WN	806	832	838		1003	1077	1175		1576	1599	1670
Soln WN	805		959	1002	1077	1175	1249	1275	1600	1677	3065
21 Neat WN	372		873	1033	1089	1170	1200		1320	1450	1590
Cell WN		791	872	1318					1519	1591	1657
Soln WN	689	792	873		1087	1171	1197		1319		1593
22 Neat WN	767	1092	1249	1265	1354	1422	1446	1593	1684	3074	
Cell WN	768	952		1262			1450	1593	1677	3078	
Soln WN	768							1595	1684	3080	
23 Neat WN	772	1058	1163	1221	1253	1326	1456	1590	1607	3076	
Cell WN	775						1584	1611	3076		
Soln WN	775	1054					1584	1613	3077		
24 Neat WN		753	766	1203	1262	1348	1420	1453	1593	1686	3080
Cell WN	735		766	1203	1265	1336	1421	1594	1689	3078	
Soln WN		767		1273	1247			1595	1695	3081	
25 Neat WN	703	766	872	1028	1188	1267	1315	1454	1608	3077	
Cell WN		766	871			1265		1454	1608	3076	
Soln WN	702	766	868		1193	1270	1317	1456	1611		
26 Neat WN	359	465	560	713	792	921	1288	1379	1616	3065	
Cell WN				713	791	922		1614	3062		
Soln WN		464	566	713	793	924	1288	1380	1616		
27 Neat WN	374		739	765	1027	1189	1265	1335	1455	1609	3076
Cell WN			720	739	765			1456	1608	3076	

	Soln W/N	554	716	739	766	1263	1326	1611	
28	Neat W/N	326	373	497	547	726	791	1607	3068
	Cell W/N			547	725	790		1606	3065
	Soln W/N		497	546	726	790	904	1380	1760
29	Neat W/N	637	820	844	1178	1211	1247	1613	3012
	Cell W/N	637	820	843	1178			1587	1611
	Soln W/N	637	819	845	1178	1210	1249	1302	3072
30	Neat W/N	306	386	561		796	1037	1271	1450
	Cell W/N				777	795		1449	1613
	Soln W/N		567	699	736	778	797	1275	1614
31	Neat W/N	370	559	748	796	1184	1293	1452	1614
	Cell W/N		649	747	796			1612	1638
	Soln W/N		568	747	796	1293		1613	1640
32	Neat W/N	345	386	741	807	918	1181	1206	1286
	Cell W/N		741	800				1599	1689
	Soln W/N		742	799	920		1281	1599	1690
33	Neat W/N	354	503	761	1117	1248	1277	1345	1578
	Cell W/N		640	762	789		1278	1443	1588
	Soln W/N	520	640	763	1132	1159	1281	1460	1607
34	Neat W/N	430			813	1154	1172	1267	1431
	Cell W/N	634	732	784	811		1186	1435	1455
	Soln W/N	416	633	731	812	1191	1273	1294	1595
35	Neat W/N	292	384	803	1033	1198	1321	1369	1446
	Cell W/N		702	805		1334		1516	1595
	Soln W/N		700	803		1329		1596	1688
36	Neat W/N	430		1106	1143	1251	1276	1333	1460
	Cell W/N		812				1331	1460	1512
	Soln W/N	416	521	812	1146		1332	1514	1589
37	Neat W/N	799	864	1171	1212	1259	1281	1306	1447
	Cell W/N	800	861	1172	1207	1264		1444	1604
	Soln W/N	801	860	1171	1206	1264		1587	1607
38	Neat W/N	309	391		842	1131	1166	1287	1314
	Cell W/N		639	830	846			1521	1608
	Soln W/N		639	828	847	1165	1285	1593	1611
39	Neat W/N	364	397	523		993	1148	1221	1332
	Cell W/N			756	786			1331	1456
	Soln W/N			785		1146		1331	1589
40	Neat W/N	382	798		988	1096	1203	1278	1336
	Cell W/N	796						1332	1455
	Soln W/N	796	894	980	1093		1333	1584	1662

^aWN is wavenumber

RESULTS AND DISCUSSION

Structures of models shown in Fig. 1 consist of various inter-unit linkages, substituents and functional groups found in lignin. The models collectively represent aliphatic and phenolic OH, C=O, CHO, COOH, CH₃, OCH₃, α,β C=C, furan, and interunit C-O-C and C-C linkages. In addition, there are models that contain more than 1 group of the same kind in their structure (e.g., models 7, 16, 19, 20, 22-24 contain at least 2 phenyl groups).

In neat state, model spectra were obtained using both near-IR Raman and FT-IR, whereas models in solution and on cellulose were analyzed only by Raman. From the model spectra obtained in three different environments, 10 most prominent Raman bands were selected for listing in Table 1. In general, due to low concentration of the models, sampling in the solution and on cellulose resulted in fewer than 10 bands.

Raman vs. IR

As is well known, Raman and IR are complementary vibrational spectroscopic techniques. This aspect was illustrated in the present study as well. In neat state, of the total detected Raman bands, only about 60% were also detected in the IR, implying that 40% of the bands could only be detected by Raman. Moreover, there were band intensity differences between the two techniques. Therefore, to obtain the most detailed chemical information, both IR and Raman analyses should be carried out.

Effect of the Environment

When models were sampled in solution and on cellulose, several Raman band positions shifted compared to the value in the neat state. A Table summarizing this data is not shown here due to lack of space but bands were classified according to the extent of the shift. Shifts between 3 and 5 cm⁻¹ were designated as small, 5 and 9 cm⁻¹ as medium and more than 9 cm⁻¹ as large. Total numbers of bands in small, medium, and large categories were, respectively, 48, 47 and 24. Considering that some of the functional groups are capable of H-bonding in solution and with cellulose, shifts associated with the bands of such groups can be readily explained. On the other hand, there were several instances where band shifts are not easily interpreted.

Band Intensity Differences

1510, 1600, and 3070 cm⁻¹ phenyl group modes

In the Raman spectra of models in neat state, a weak 1510 cm⁻¹ band was detected. However, in solution, for most models, this band was not detected. On the contrary, the 1600 cm⁻¹ band was strong in both states. The intensities of the 1600 (aromatic ring stretch) and 3070 (aromatic C-H stretch) cm⁻¹ bands varied significantly among the models (Figs. 2 and 3). Bar-plot in Fig. 2 shows the variation of the molar intensity of the 1600 cm⁻¹ band. The intensities are plotted with respect to the 1600 cm⁻¹ band intensity of model 26 which had the lowest non-zero value.

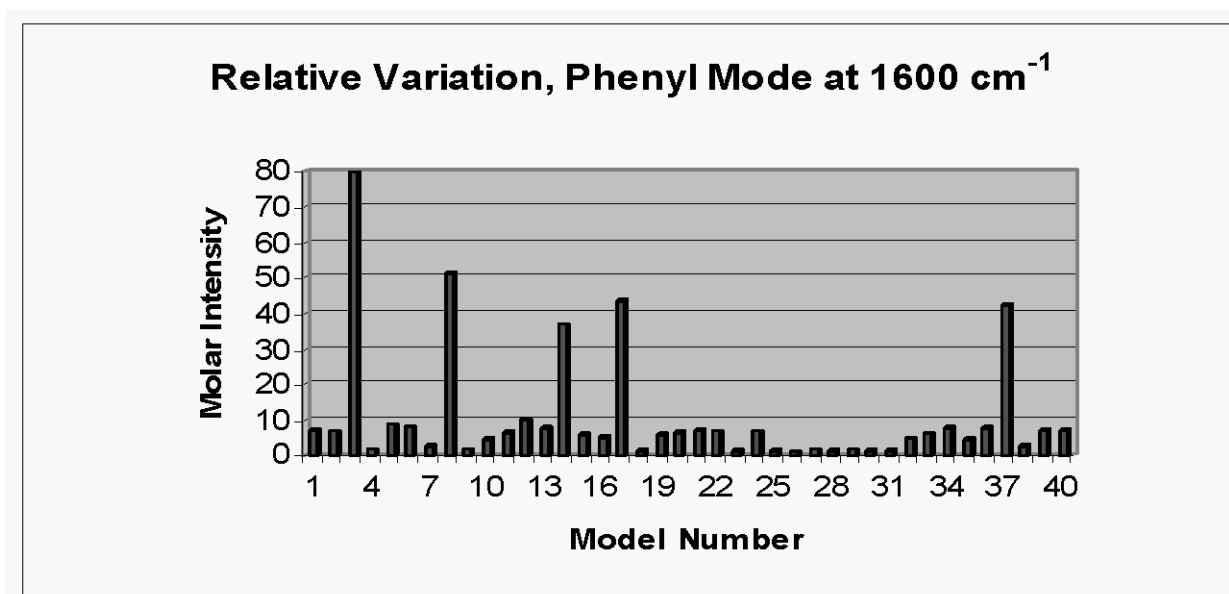


Fig. 2: Relative variation of molar intensity of the ≈ 1600 cm⁻¹ phenyl mode in lignin models. Intensity variation is with respect to model 26 whose intensity was set to 1. See Fig. 1 for identifying various lignin models.

Previously, such intensity variation was observed [9] when a number of models were investigated by conventional Raman spectroscopy (514.5 nm laser excitation). As discussed earlier [9], the 1600 cm^{-1} band intensity enhancement was reported to be due to both pre-resonance Raman and conjugation effects. Considering the long wavelength nature (1064 nm) of the laser excitation in the present work, which makes excitation far removed from any electronic absorption in the models, the pre-resonance Raman is not expected to play a role in intensity enhancement. Therefore, the intensity of the aromatic band at 1600 cm^{-1} is affected solely by the π -electron conjugation between the phenyl ring and its substituents. More conjugation and consequently, more conjugation-enhancement is usually present in

the absence of steric hindrance from substituents on the 2 and 6 positions of the phenyl ring.

While the intensity was very sensitive to the model structure, the position of the 1600 cm^{-1} Raman band was found to be only minimally sensitive. In about 70% of the models, including those containing more than one phenyl group, the vibrational frequency was confined between 1594 to 1603 cm^{-1} (Table 1).

A similar molar intensity variation plot was generated for the 3070 cm^{-1} band. For this aromatic C-H stretch mode, the intensities were calculated relative to that of model 29, which had the lowest non-zero intensity in solution. The models with missing data in the plot are those whose spectra did

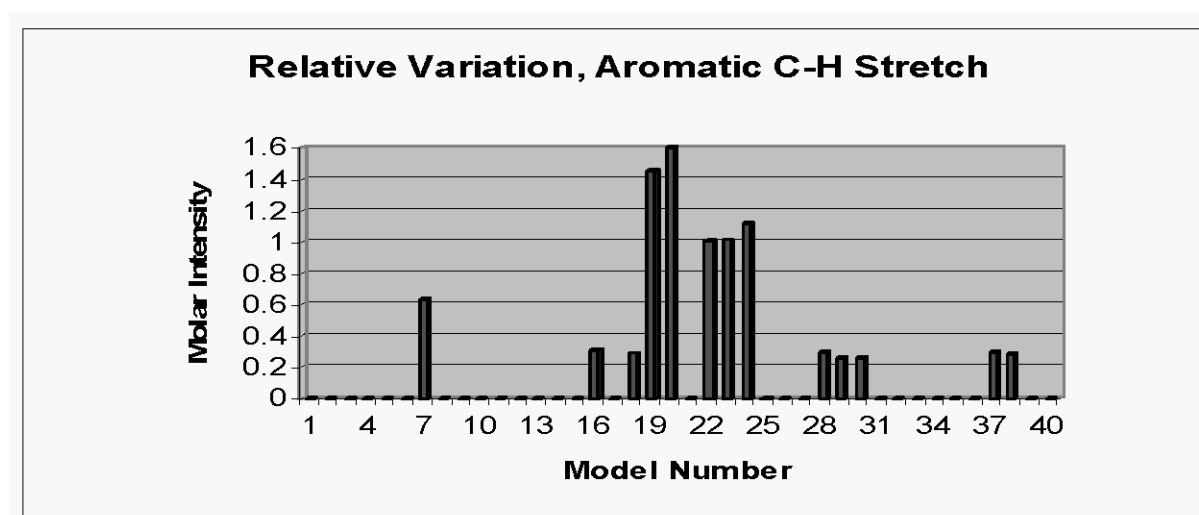


Fig. 3: Relative variation of molar intensity of the $\approx 3070 \text{ cm}^{-1}$ C-H stretch in lignin models. Intensity variation is with respect to model 29 whose intensity was set to 1. See Fig.1 for identifying various lignin models.

When Figs. 2 and 3 are compared, it is noted that the two model sets that produced intensity enhancements are different. This suggests that the mechanisms underlying the 1600 and 3070 cm^{-1} band enhancements are not the same.

Raman Frequencies and Band Assignment

Making assignments of characteristic Raman frequencies of the model compounds is a complex task and the already available information in the literature is extremely helpful [9-11]. Using existing knowledge, bands in model spectra were identified that were characteristic of various sub-structures/groups (Table 2). Column 1 in Table 2 identifies the group, and corresponding Raman frequencies are listed in the subsequent columns according to various model characteristics. For

instance, depending upon the substitution pattern of the phenyl group (mono, di, tri or tetra) aromatic bands may or may not be seen in specific regions of the spectrum. On the other hand, functional and substituent groups have no such limitation and they are usually detected in their respective regions.

In lignin models, there are some phenyl group modes of vibrations that are substituent sensitive and others that are not. The former are coupled to the motions of the substituent group and their frequencies move about significantly depending upon the nature of the substituent. These modes are not useful in characterizing the phenyl group. However, the substituent-insensitive frequencies show variation that is much more limited and these can be taken to be the characteristic vibrations of the phenyl group.

Table 2: Raman Frequencies of selected sub-structures in models

Group	Model Characteristics/Vibrational Modes			
Phenyl	Mono-sub.	Di-sub.	Tri-sub., all are 1, 3, 4 type	Tetra-sub., 1, 3, 4, 5 type
	615-618	Ortho, 639-643 (IPRD)	616-727 (IPRD)	609-629 (IPRD)
	1000-1003	Para, 635-673 (IPRD)	1141-1198 (C-H IPBM)	1148-1203
	Both are in plane ring deformations (IPRD)	Ortho, 1053-1058 (C-H in plane bending mode)	1261-1293, CC stretch	(IPBM)
	1449-1454	Para, 995-1023 (C-H IPBM)	1426-1464, CC stretch	1332-1432
	CC stretch		1498-1520, CC stretch	CC stretch
	1597- 1600	Ortho, 1430-1465, CC str	1570-1590, CC stretch	1452-1517
CC stretch	Para, 1400-1420, CC str	1590-1614, CC stretch	CC stretch	
	Ortho, 1455-1510, CC str		1578-1597	
	Para, 1480-1525, CC str		CC stretch	
	ortho & para, 1580-1605			
	CC stretch			
Aromatic C-H	3061-3090, C-H str			
C=O^a	α (e.g., 5)	α -O-1 (e.g., 7)	β -O-1 (22)	4-O-C (10)
C=O stretch	1650-1681	1727	1684-1687	1740, 1763
HC=O	1 (12)	β (3)		
C=O stretch	1664-1684	1664, 1675		
HO-C=O	1 (1)	β (8)		
C=O stretch	\approx 1695 (soln)	\approx 1690 (soln)		
α, β HC=CH	899-982	1271-1313	1621-1654	3017-3035
	Trans C-H wag	Trans C-H sym. rock	C=C stretch	C-H stretch
H₂C-OH	373-463	767-922	995-1053	1247-1433
	C-C-O bend	In phase C-C-O stretch	Out of phase C-C-O stretch	C-O-H bend
HC-OH	516-519	845-872	1027, 1028	1157-1163
	C-C-O bend	In phase C-C-O stretch	Out of phase C-C-O stretch	1267-1315
				C-O-H bend
O-CH₃	1143-1209	1426-1470		
	Rock	Deformation		
Furan	1430	1498	1597	
	C-O-C in phase stretch	In phase C=C stretch	Out of phase C=C stretch	

^aLocation of the C=O is indicated by the α , α -O-1, β -O-1, and 4-O-C, model example is in parentheses

Considering the limitation of space, a detailed discussion of the Raman frequencies and their assignments is not possible here. Nevertheless, it is important to note that a large number of previously identified lignin and DHP Raman bands were detected in the spectra of this current set of models.

REFERENCES

- Ona, T., Sonoda, T., Ito, K., Shibata, M., Kato, T., and Ootake, Y., *J. Wood Chem. Technol.* 17(4), 399(1997).
- Agarwal, U.P., *J. Wood Chem. Technol.* 18(1-2), 381(1998).
- Agarwal, U.P. and Akhtar, M., *Proc. 2000 TAPPI Pulping, Process, and Product Quality Conf.*, pp 1-12.
- Lavine, B.K., Davidson, C.E., Moores, A.J., and Griffiths, P.R., *Applied Spectroscopy* 55, 960(2001).
- Proniewicz, L.M., Paluszkiwicz, C., Weselucha-Birczynska, A., Baranski, A., and Dutka, D., *J. Mol. Struct.* 614, 345(2002).
- Saariaho, A.-M., Hortling, B., Jaaskelainen, A.-S., Tamminen, T., and Vuorinen, T., *J. Pulp Paper Sci.* 29(11), 363(2003).
- Agarwal, U.P., Weinstock, I.A., and Atalla, R.H., *Tappi J.*, 2(1) 22(2003).
- Agarwal, U.P. and Landucci, L.L., *J. Pulp Paper Sci.* 30(10), 269(2004).
- Agarwal, U.P., in *Advances in Lignocellulosic Characterization*, Ed. D.S. Argyropoulos, TAPPI Press, Atlanta, GA, 1999, pp 209.
- Lin-Vien, D., Colthup, Norman B., Fateley, W.G., and Grasselli, J.G., *The Handbook of Infrared and Raman Characteristic Frequencies of Organic Molecules*: Academic Press, CA, 1991.
- Ehrhardt, S.M., *An Investigation of the Vibrational Spectra of Lignin Model Compounds*, Ph.D. Thesis Dissertation, 1984, Institute of Paper Science and Technology, Atlanta GA.

In: Proceedings of the 59th APPITA Annual Conference and Exhibition incorporating the 13th ISWFPC (International Symposium on Wood, Fibre, and Pulping Chemistry), held in Auckland, New Zealand (May 16-19, 2005). [Carlton, Victoria, Australia]: APPITA, c2005. Both print and CD versions are available. pp. 1-8.